Intense polar temperature inversion in the middle atmosphere on Mars

Article *in* Nature Geoscience · October 2008

DOI: 10.1038/ngeo332 · Source: OAI

19 authors, including:

N. G. Heavens
Hampton University
73 PUBLICATIONS **592** CITATIONS
SEE PROFILE

P. G. J. Irwin
University of Oxford
358 PUBLICATIONS **5,269** CITATIONS
SEE PROFILE

Stephen R. Lewis
The Open University (UK)
256 PUBLICATIONS **2,982** CITATIONS
SEE PROFILE

Peter L. Read
University of Oxford
364 PUBLICATIONS **5,089** CITATIONS
SEE PROFILE

Intense polar temperature inversion in the middle atmosphere on Mars

D. J. McCLEESE[1]*, J. T. SCHOFIELD[1], F. W. TAYLOR[2]*, W. A. ABDOU[1], O. AHARONSON[3], D. BANFIELD[4], S. B. CALCUTT[2], N. G. HEAVENS[3], P. G. J. IRWIN[2], D. M. KASS[1], A. KLEINBÖHL[1], W. G. LAWSON[3], C. B. LEOVY[5], S. R. LEWIS[6], D. A. PAIGE[7], P. L. READ[2], M. I. RICHARDSON[3], N. TEANBY[2] AND R. W. ZUREK[1]

[1]Jet Propulsion Laboratory, California Institute of Technology, Pasadena, California 91103, USA
[2]Department of Physics, University of Oxford, Clarendon Laboratory, Oxford OX1 3PU, UK
[3]Division of Geological and Planetary Sciences, California Institute of Technology, Pasadena, California 91105, USA
[4]Department of Astronomy, Cornell University, Ithaca, New York 14850, USA
[5]Department of Atmospheric Sciences, University of Washington, Seattle, Washington 98101, USA
[6]Department of Physics and Astronomy, Open University, Milton Keynes MK7 6AA, UK
[7]Department of Earth and Space Sciences, University of California, Los Angeles, California 90024, USA
*e-mail: Daniel.J.McCleese@jpl.nasa.gov; fwt@atm.ox.ac.uk

Published online: 12 October 2008; doi:10.1038/ngeo332

Current understanding of weather, climate and global atmospheric circulation on Mars is incomplete, in particular at altitudes above about 30 km. General circulation models for Mars[1–6] are similar to those developed for weather and climate forecasting on Earth and require more martian observations to allow testing and model improvements. However, the available measurements of martian atmospheric temperatures, winds, water vapour and airborne dust are generally restricted to the region close to the surface and lack the vertical resolution and global coverage that is necessary to shed light on the dynamics of Mars' middle atmosphere at altitudes between 30 and 80 km (ref. 7). Here we report high-resolution observations from the Mars Climate Sounder instrument[8] on the Mars Reconnaissance Orbiter[9]. These observations show an intense warming of the middle atmosphere over the south polar region in winter that is at least 10–20 K warmer than predicted by current model simulations. To explain this finding, we suggest that the atmospheric downwelling circulation over the pole, which is part of the equator-to-pole Hadley circulation, may be as much as 50% more vigorous than expected, with consequences for the cycles of water, dust and CO_2 that regulate the present-day climate on Mars.

We report new observations of the thermal structure of the martian atmosphere that investigate the global atmospheric circulation, and show that the meridional component is significantly faster than previously realized. The data are from the Mars Climate Sounder (MCS), an infrared radiometer of advanced design[8], optimized for remote sounding of the martian atmosphere from orbit in one broadband visible and eight infrared channels in the 0.3 to 50 μm spectral range. MCS routinely uses the limb-scanning technique to achieve half-scale height resolution (~5 km) in temperature and aerosol retrievals that extend from near the surface to 80 km. This resolution and range are significant improvements for global monitoring of the martian atmosphere. Direct temperature measurements from descent vehicles have high vertical resolution and coverage, which has shown a wealth of interesting detail, but are very limited in global coverage. Radio-occultation soundings have high vertical resolution but occur only twice per orbit and are limited to the lowest 30 km or so of the atmosphere.

MCS observations are made from the Mars Reconnaissance Orbiter[9] (MRO), which has been in a near-circular sun-synchronous polar orbit around Mars at a median altitude of 265 km since September 2006. The viewing geometry from the orbit of MRO includes excellent coverage of the south polar region, which was experiencing the permanent darkness of winter at the time that observations began. The sun-synchronous orbit yields essentially meridional tracks of limb observations, making it possible to create latitudinal cross-sections of the temperature structure as a function of pressure or height. The example in Fig. 1 shows the expected trend at low altitudes of temperature increasing from pole to equator owing to solar heating, but also captures several aspects of the complex meteorology of the martian southern winter polar region.

An important feature of the cross-section in Fig. 1 is the large temperature inversion in the middle atmosphere over the south pole. Such a warming in the winter polar region is suggested in earlier infrared observations of Mars by Mariner 9 (ref. 10) and Viking[11], but retrievals from these primarily nadir observations do not extend high enough (typically being limited to $\leqslant$35 km) to capture the peak or higher structure of the warming. The Mars Global Surveyor Thermal Emission Spectrometer (MGS-TES) limb–nadir retrievals extend high enough to include the lower part of the warming, but do not observe the region of maximum heating[12]. Furthermore, although a polar warming is a prominent feature in general circulation models of the martian atmosphere[1–6], the amplitude and poleward extent of the temperature inversion has generally been

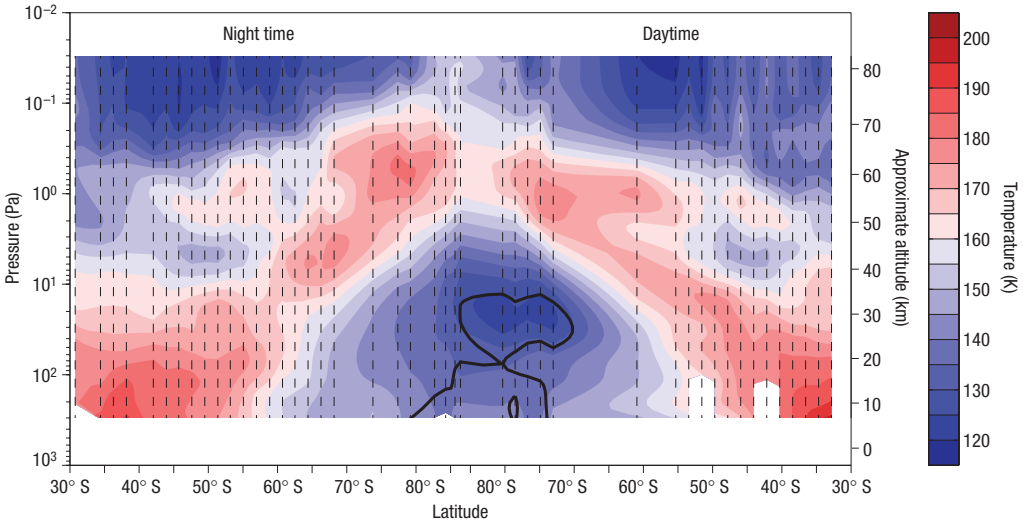

Figure 1 A cross-section of the atmospheric temperature in the southern hemisphere of Mars for mid-southern winter ($L_s = 136°$, 16 Nov 2006). The cross-section is composed from successive MCS limb retrievals (indicated by vertical dashed lines) that extend from the nightside to the dayside (left-to-right), with a mean local time of 03:16 LST to 15:36 LST at 30° S. Latitudes polewards of 70° S receive no solar heating; latitudes polewards of 55° S are covered by seasonal CO_2 frost. The latitude of closest approach to the pole is ~86.5° S, owing to the inclination of the sun-synchronous MRO orbit. The dark black contours indicate the CO_2 frost point.

predicted to be significantly (10–30 K) smaller than is seen in the MCS data.

Winds will increase with height in the region of strong horizontal temperature gradients that surround the large mass of cold air over the pole, and this defines the polar vortex. At higher altitudes, the latitudinal temperature trend reverses, giving the polar temperature inversion seen in Fig. 1 and a decrease with height in the strength of the zonal winds. This spatially correlated atmospheric trend is consistent with the behaviour of a Hadley circulation in which the polar warming is the result of compressional heating in the descending branch of the mean meridional overturning circulation. The dynamical origin of the warming is assured by the absence of solar heating in the winter polar night. Figure 2 shows some individual vertical profiles of temperature from a 20-sol interval, $L_s = 130°$–$140°$ ($L_s = 90°$ represents the southern winter solstice). These profiles lie in an annulus between 70° S and 75° S, just outside the polar night, but still within the seasonal CO_2 cap, which extends to about 55° S at this time of year. This annulus is a region of relatively low dust and ice cloud opacity, making the retrievals of temperature simpler and more accurate (typically ±2 K, see the Methods section). In the lowest two scale heights (the vertical e-folding distance for pressure, ~10 km for Mars), the profiles follow the atmospheric frost-point temperature quite closely, although they were not constrained to do so by the retrieval process. Above about 20 km, the pronounced temperature inversion begins, with maximum temperatures near 50 km altitude reaching as much as 60 K above the surface value.

Figure 3 compares the structure of the middle-atmospheric warming revealed by the MCS data with profiles for the same time and season taken from the Mars Climate Database (MCD). This is a compendium of model simulations that has been shown[3,4,7] to reproduce the major features of the diurnal and seasonal behaviour of the martian atmosphere as it was known before the first MCS observations. As a readily available public resource, MCD serves as a *de facto* community reference model: it is commonly used for model intercomparisons, it is commonly cited in the open literature and its published components are often used in other models. When the vertical temperature profiles from MCS and the MCD are averaged over $L_s = 120°$–$150°$, both show temperature maxima in the polar middle atmosphere; however, the peak warming in MCS data is about 20 K higher (180 K versus 160 K) and about 15° latitude further poleward. The magnitude of the temperature inversion is also markedly larger in MCS data (35 K) compared with the MCD (15 K), indicating that the martian Hadley circulation is more vigorous than current models predict.

Such strong downward motion over the polar cap requires strong poleward flow aloft, and powerful momentum sinks due to zonally asymmetric wave forcing (commonly known as wave drag) are required to balance the Coriolis force acting on the flow[3]. In Earth's upper mesosphere, internal gravity waves provide most of the wave drag needed to simulate warm winter poles; in the stratosphere, the wave drag and polar warming can be produced by dissipating (breaking) planetary waves[13]. Internal gravity waves, planetary waves and atmospheric thermal tides may contribute on Mars[14–16]. The thermal tides could contribute to the polar warming by providing sufficient momentum flux divergence to extend the meridional circulation right up to the winter pole[17]. Thermal tides should certainly be strong on Mars, because of the very large diurnal temperature swing at the surface, and their presence has been inferred at high altitudes from probe landing profiles, where day-entry and night-entry differences have been interpreted as due to tides[18].

A comparison of dayside and nightside retrievals from a set of profiles measured by MCS under low-dust conditions reveals the vertical structure of the thermal tide in the martian lower and middle atmosphere (Fig. 4). Unlike the Earth, the thermal tide is the dominant wave mode in the martian atmosphere, and gives rise to much of the variance of wind and pressure measured at the surface. The peak-to-peak amplitude of the diurnal thermal tide observed by MCS at roughly 45–50° N in the northern plains in late northern summer is in excess of 20 K at 1 Pa, with an observed vertical wavelength of 4–5 scale heights. The latter is in good agreement with the expectation from classical tidal theory and from numerical models[2], and the observed amplitude of the tide is consistent with it being an important component of the inferred very energetic meridional circulation presented here. The

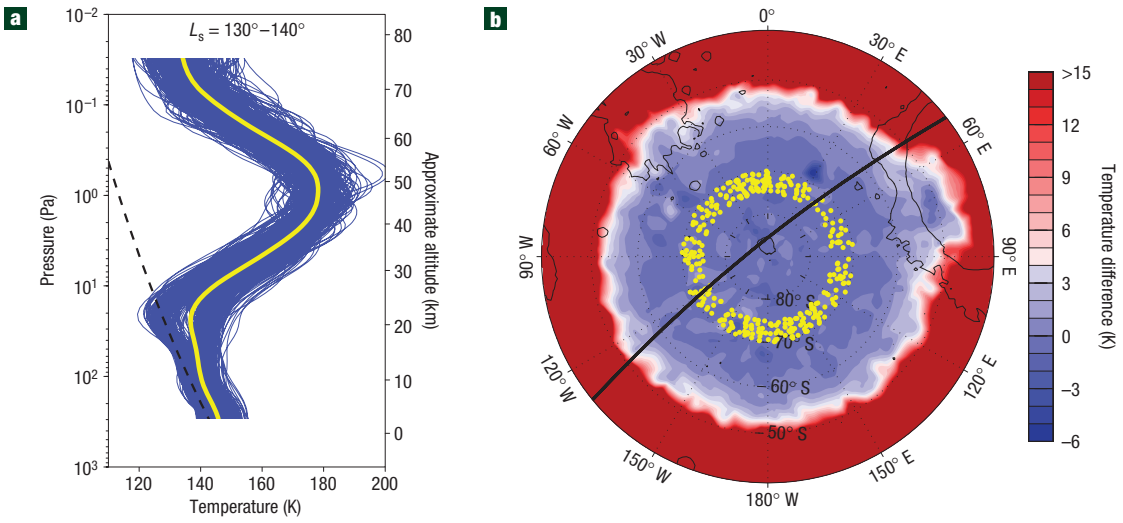

Figure 2 Individual temperature profiles near the south pole. a, 344 profiles of temperature from near-polar latitudes (70°–75° S) for mid-southern winter (L_s = 130°–140°). The black dashed line indicates the CO_2 frost point. **b**, Yellow dots mark the locations of the profiles on a polar map of the day–night difference in surface brightness temperature (31.7 μm). The colour bar saturates for temperature differences >15 K to illustrate the extent of the seasonal CO_2 ice cap. The black contours indicate topography every 4 km, and the solid black line crossing near the pole is the sub-orbital track corresponding to the transect shown in Fig. 1.

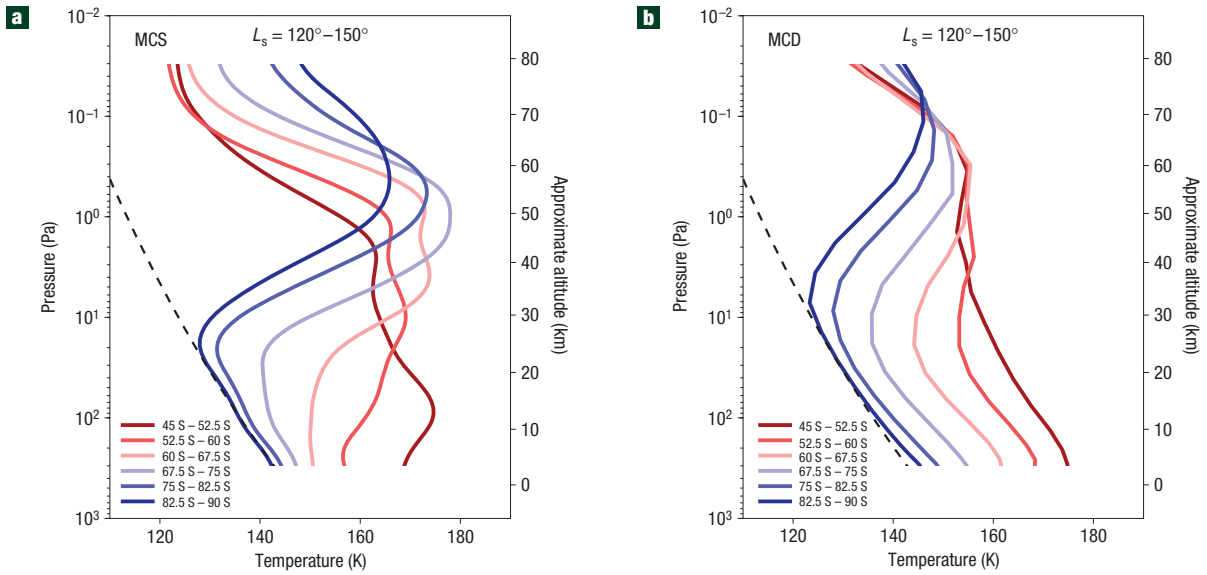

Figure 3 Comparison of measured and model-generated temperature profiles. a, Measured mean vertical profiles of atmospheric temperature at latitudes from 90 to 45° S, in 7.5° latitude bins, including all soundings (day and night) within L_s = 120°–150°. The black dashed line shows the CO_2 frost point. **b**, Model-generated profiles from the MCD (version 3, 'Martian Year 24 dust and average solar flux scenario,' Mars Month 5) (refs 3,4) for the same conditions as the measurements in **a**. Only profiles with LST between 02:00 and 04:00 and 14:00 and 16:00 were included in the averages, to allow direct comparison with the MCS profiles.

large variability, on a relatively short seasonal timescale, between the individual temperature profiles shown in Figs 2 and 4 also suggests an important role for gravity waves and eddies[6].

Gravity wave activity and tidal amplitudes depend on the solar heating distribution, which, in turn, is sensitive to the distribution and properties of dust and clouds[19,20]. Variation in the column optical depth or the distribution of opacity within the column can significantly change the vigour of the global circulation[1,21,22]. Although the column global dust opacity has been frequently observed, its vertical distribution has been only roughly estimated using limited Viking limb observations and Mariner 9 camera observations[23,24]. Improved model simulations of the strong middle-atmosphere polar warming now observed require improved knowledge of the vertical distribution of dust,

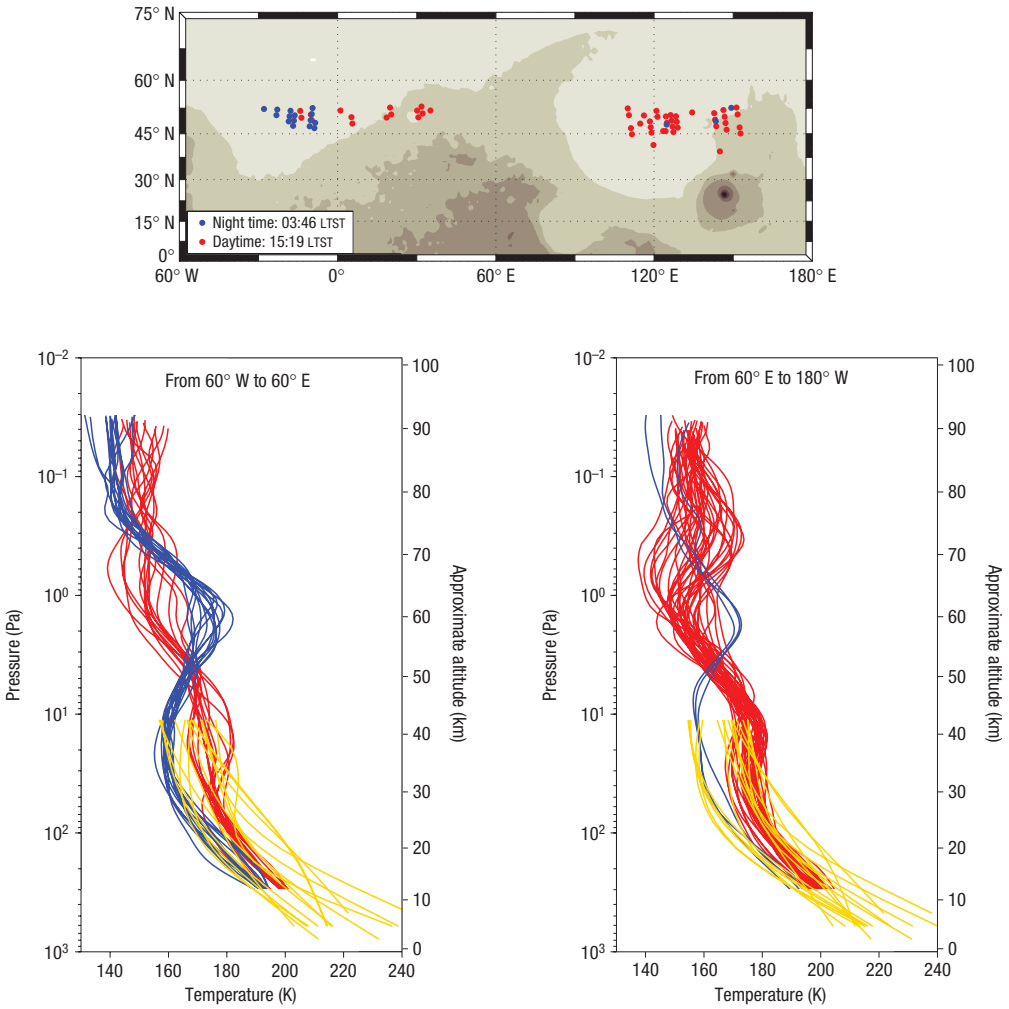

Figure 4 Tidal and gravity wave structure in vertical temperature profiles for northern mid-latitudes (35° N to 53° N) between $L_S = 150°$ and 170°. Blue lines correspond to night time (03:46) and red lines to daytime (15:19), in the two different longitude groups (−60° to +60°, and +60° to +180°) shown in the upper panel. The diurnal thermal tide can be seen clearly in the day–night differences. Profiles within the same latitude, longitude and L_S ranges, measured at 14:30 local time by the MGS-TES instrument[12] are shown for reference (gold lines). Owing to differences in viewing geometry, the TES (nadir viewing) profiles are limited to below 40 km, and MCS (limb viewing) profiles are reliable above 10 km.

which can be obtained from further analysis of MCS observations. We also note that a more vigorous meridional circulation will tend to exacerbate the problem of obtaining agreement between current models and observations of the seasonal water vapour budget on Mars. Thus, future investigations of systematic model error for temperature, dust and water vapour using MCS measurements should lead to major improvements in our ability to simulate the martian climate system.

METHODS

RADIANCE SPECTRA

All MCS retrievals reported here are based on limb observations from a period of nominal limb–nadir scanning of the atmosphere between September 2006 and January 2007. MCS has eight mid- and far-infrared channels and one visible/near-infrared channel covering key features of martian atmospheric spectra. Three channels in the 15 μm CO_2 absorption band are used for both temperature and pressure retrieval. The 22 μm dust absorption band and the 12 μm water-ice absorption feature provide aerosol information. Each channel consists of 21 detectors, which observe the atmosphere simultaneously. Their angular separation provides a vertical resolution of ~5 km at the Mars limb.

RETRIEVAL ALGORITHM AND RADIATIVE TRANSFER CALCULATIONS

The retrieval algorithm is a modified Chahine scheme[25], which uses iterative radiative transfer simulations to fit the observed radiances. Pressure, temperature, dust and water ice are retrieved simultaneously. Results agree well with the output of a retrieval scheme based on the optimal estimation method[26]. Radiative transfer for the gases (CO_2 and H_2O) is based on the HITRAN 2004 line list[27]. A Curtis–Godson approximation with precalculated transmissions for each channel is used. Errors introduced owing to the approximation are generally below 1% for the mid-infrared channels in typical martian atmospheric conditions. No scattering parameterization has been implemented at this stage for aerosols. Both dust and water-ice absorptions are described by extinction efficiencies derived from Mie calculations spectrally integrated for each channel. The Mie calculations for dust assume a gamma distribution with an effective particle radius of 1.54 μm and are based on the refractive indices for Mars dust by Wolff *et al.*[28]. For the water-ice Mie calculations, a gamma distribution with an effective particle radius of 1.36 μm was used, with refractive indices taken from Warren[29].

ERRORS AND UNCERTAINTIES

Theoretical analyses of the MCS retrievals, based on instrument noise measurements and test retrievals from synthetic data, indicate that the individual retrieved temperature profiles are reliable to within 2 K for most atmospheric conditions with low or moderate dust loadings[8,30]. Comparison of Fig. 1 and similar cross-sections of MCS data with those obtained for similar seasons from combined limb and nadir observations by the MGS-TES (see Plate 5 of ref. 12) also show generally very good agreement where they overlap, despite being four Mars years apart (this season (southern winter) shows the least interannual variability). Aerosol opacity profiles are subject to extra uncertainties due to variations in composition, particle size and shape, and are still under development. Likewise, accurate dust, as well as temperature, retrievals are a prerequisite for deducing useful water vapour profiles and the latter are still being evaluated.

Received 16 June 2008; accepted 16 August 2008; published 12 October 2008.

References

1. Haberle, R. M. *et al.* Mars atmospheric dynamics as simulated by the NASA/Ames general circulation model. *J. Geophys. Res.* **98**, 3093–3124 (1993).
2. Wilson, R. J. & Hamilton, K. P. Comprehensive model simulation of thermal tides in the Martian atmosphere. *J. Atmos. Sci.* **53**, 1290–1326 (1996.).
3. Forget, F. *et al.* Improved general circulation models of the Martian atmosphere from the surface to above 80 km. *J. Geophys. Res.* **104**, 24155–24175 (1999).
4. Lewis, S. R. *et al.* A climate database for Mars. *J. Geophys. Res.* **104**, 24177–24194 (1999).
5. Richardson, M. I., Toigo, A. D. & Newman, C. E. A general purpose, local to global numerical model for planetary atmospheric and climate dynamics. *J. Geophys. Res.* **112**, E09001 (2007).
6. Medvedev, A. S. & Hartogh, P. Winter polar warmings and the meridional transport on Mars simulated with a general circulation model. *Icarus* **186**, 97–110 (2007).
7. Read, P. L. & Lewis, S. R. *The Martian Climate Revisited* (Springer-Praxis, 2004).
8. McCleese, D. J. *et al.* Mars Climate Sounder: An investigation of thermal and water vapor structure, dust and condensate distributions in the atmosphere, and energy balance of the polar regions. *J. Geophys. Res.* **112**, doi:10.1029/2006JE002790 (2007).
9. Zurek, R. W. & Smrekar, S. J. An overview of the Mars Reconnaissance Orbiter (MRO) science mission. *J. Geophys. Res.* **112**, doi:10.1029/2006JE002701 (2007).
10. Conrath, B., R. *et al.* Atmospheric and surface properties of Mars obtained by infrared spectroscopy on Mariner 9. *J. Geophys. Res.* **78**, 4267–4278 (1973).
11. Jakosky, B. & Martin, T. Z. Mars: North-polar atmospheric warming during dust storms. *Icarus* **72**, 528–534 (1987).
12. Smith, M. D., Pearl, J. C., Conrath, B. J. & Christensen, P. R. Thermal Emission Spectrometer results: Mars atmospheric thermal structure and aerosol distribution. *J. Geophys. Res* **106**, 23929–23945 (2001).
13. Andrews, D. G., Holton, J. R. & Leovy, C. B. *Middle Atmosphere Dynamics* (Academic, 1987).
14. Creasey, J. E., Forbes, J. M. & Hinson, D. P. Global and seasonal distribution of gravity wave activity in Mars' lower atmosphere derived from MGS radio occultation data. *Geophys. Res. Lett.* **33**, L01803 (2006).
15. Barnes, J. R. Possible effects of breaking gravity waves on the circulation of the middle atmosphere of Mars. *J. Geophys Res.* **95**, 1401–1421 (1990).
16. Zurek, R. W. & Haberle, R. M. Zonally symmetric response to atmospheric tidal forcing in the dusty Martian atmosphere. *J. Atmos. Sci.* **45**, 2469–2485 (1988).
17. Wilson, R. J. A general circulation model simulation of the Martian polar warming. *Geophys. Res. Lett.* **24**, 123–126 (1997).
18. Seiff, A. & Kirk, D. B. Structure of the atmosphere of Mars in summer at mid-latitudes. *J. Geophys. Res.* **82**, 4364–4378 (1977).
19. Hinson, D. P. & Wilson, R. J. Temperature inversions, thermal tides, and water ice clouds in the atmosphere of Mars. *J. Geophys. Res.* **109**, E01002 (2004).
20. Wilson, R. J., Lewis, S. R., Montabone, L. & Smith, M. D. Influence of water ice clouds on Martian tropical atmospheric temperatures. *Geophys. Res. Lett.* **35**, L07202 (2008).
21. Haberle, R. M., Leovy, C. B. & Pollack, J. B. Some effects of global dust storms on the atmospheric circulation of Mars. *Icarus* **50**, 322–367 (1982).
22. Schneider, E. K. Martian great dust storms: interpretive axially symmetric models. *Icarus* **35**, 302–331 (1983).
23. Anderson, E. & Leovy, C. Mariner 9 television limb observations of dust and ice hazes on Mars. *J. Atmos. Sci.* **35**, 723–734 (1978).
24. Jaquin, F., Gierasch, P. & Kahn, R. The vertical structure of limb hazes in the Martian atmosphere. *Icarus* **68**, 442–461 (1986).
25. Chahine, M. T. A general relaxation method for inverse solutions of the full radiative transfer equation. *J. Atmos. Sci* **29**, 741–747 (1972).
26. Rodgers, C. D. *Inverse Methods for Atmospheric Sounding* (World Scientific, 2000).
27. Rothman, L. S. *et al.* The HITRAN 2004 molecular spectroscopic database. *J. Quant. Spectrosc. Radiat. Transfer.* **96**, 139–204 (2005).
28. Wolff, M. J. *et al.* Constraints on dust aerosols from the Mars Exploration Rovers using MGS overflights and Mini-TES. *J. Geophys. Res.* **111**, E12S17 (2006).
29. Warren, S. G. Optical constants of ice from the ultraviolet to the microwave. *Appl. Opt.* **23**, 1206–1225 (1984).
30. McCleese, D. J. *et al.* Remote sensing of the atmosphere of Mars using infrared pressure modulator and filter radiometry. *Appl. Opt.* **25**, 4232–4245 (1986).

Acknowledgements

The authors acknowledge J. Shirley, C. Backus, T. Pavlicek and E. Sayfi for their contribution to the acquisition and analysis of MCS data. The research described in this letter was carried out at the Jet Propulsion Laboratory, California Institute of Technology, under a contract with the National Aeronautics and Space Administration and in the UK with the support of the Science, Technology and Facilities Council.

Author information

Reprints and permissions information is available online at http://npg.nature.com/reprintsandpermissions.
Correspondence and requests for materials should be addressed to D.J.M. or F.W T.